Experimental study on fatigue properties of Q420C steel welded joints at room temperature

Liguo Yang [a,b] , Yongming Xing [b]*

[a] Key Laboratory of Civil Engineering Structure and Mechanics, Inner Mongolia University of Technology, Hohhot, 010051,China. Email:76351789@qq.com

[b] School of Science, Inner Mongolia University of Technology, Hohhot, 010051, China. Email:xym@imut.edu.cn

* Corresponding author

Abstract

To evaluate the fatigue life of Q420C steel welded joints, fatigue tests were performed on butt-welded joints, cross-butt-welded joints and cross-fillet-welded joints. The fatigue strength S-N curves of the joints were fitted. Then the formation and development of fatigue cracks were analyzed by fracture morphology. The fatigue properties of joints were compared with literature data and standard curves. The results showed that the fatigue test data of the three types of welded joints were roughly above the standard curves. Moreover, the fatigue strength of butt-welded joint was significantly higher than the calculated values of standards, indicating a large safety margin. The test value of cross-butt-welded joint was close to the calculated values of standards, so it is suggested to moderately reduce the standard values. In addition, all the three standards could well predict the fatigue life of cross-fillet-welded joint. The fracture morphology of the specimens showed the development process of fatigue damage, and the fatigue displacement curve and damage curve proved the formation of the fatigue fracture in specimens.

Keywords

Butt-welded joint; Cross-butt-welded joint; Cross-fillet-welded joint; Fatigue damage; S-N curve

Graphical abstract
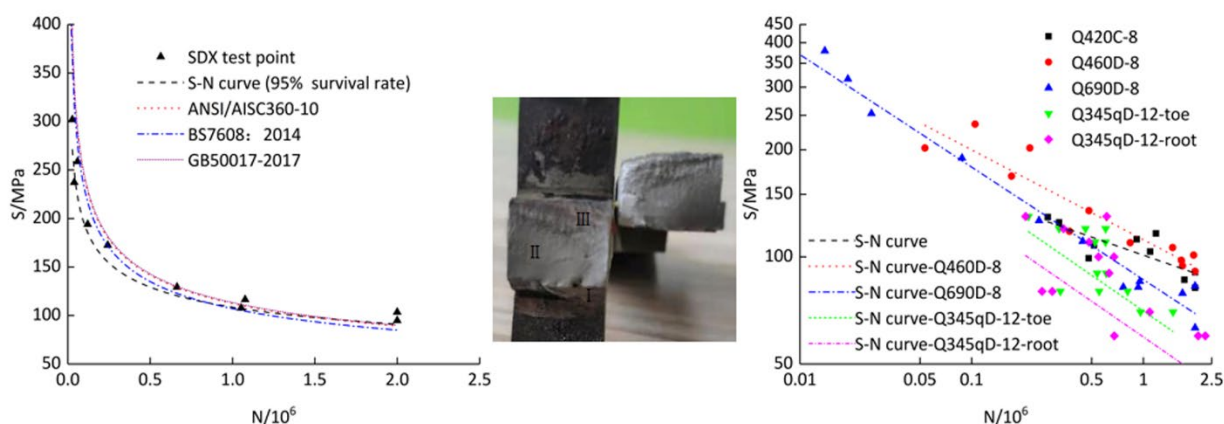
1 INTRODUCTION

With the wide application of Q420 steel in transmission towers, offshore drilling platforms and large public structures, the strength, toughness, fatigue resistance, machinability, welding performance and corrosion resistance of Q420 steel welded joints have become the focuses of structural engineers. About 80% of the failure of metal structures is resulted from the fatigue fracture of materials or connections(Lei et al., 2010). The structural deformation is quite small before fatigue fracture occurs, and no obvious macroscopic plastic deformation can be observed. But sudden fatigue damage often induces huge loss to life and property.

Many studies were carried out on the fatigue performance of various steels and welded connections. Lei et al. (2010) summarized the research progress in the fatigue of steel structures in China in the past 30 years from six aspects (fatigue load spectrum, fatigue influencing factors, fatigue failure mechanism, fatigue test methods, fatigue life estimation, and fatigue design methods), and pointed out the fatigue problems to be solved for steel structure. Jia et al. (2017) carried out static tensile test and axial tensile fatigue test respectively on standard round rod specimens and hourglass-shaped smooth specimens. They found that Q345qD butted weld had better fatigue, and the fatigue life was significantly improved with the decreasing stress, and gave the fitting formula of fatigue life with varying stress. Zong et al. (2017a, 2017b) performed fatigue tests on 26 non-bearing Q345qD steel cross-fillet welds, and plotted the S-N curve of weld leg failure and root failure. Moreover, they developed a three-dimensional mixed-mode fatigue crack propagation analysis method to compare the predicted fatigue life with the experimental one, providing a reference for the fatigue evaluation of fillet welds. Cheng et al. (2017) conducted normal temperature fatigue performance tests on ∟125×12 angle steel plates with strength grades of Q420B and Q420C, and obtained the S-N curves of the two kinds of steels. The results showed that Q420C steel had an advantage over Q420B steel in fatigue performance under the same conditions, and the test results were much higher than the value prescribed in the GB 50017-2003 standard.

Defects are inevitable in the welding process. Adjusting the welding process or adopting post-weld treatment can improve the fatigue performance of the weld. Janosch et al. (1996) studied the fatigue properties of four steels (Domex350, Domex590, Weldox700 and Weldox900) with steel strength variation after weld treatment. Custafsson (2002) tested the effect of thickness change on the fatigue performance of the 3~12mm thick Domex550 MC, a high-strength steel, through cross-welded joints. The study showed that the fatigue performance decreased with the increasing plate thickness. Weich I (2008) studied the impact of post-weld treatment on the fatigue properties of S355J2 and S690QL steels. Leitner M et al. (2011) analyzed the influence of welding process and high-frequency shot peening technology on the fatigue properties of S960 steel. Okawa T et al. (2013) investigated the impact of different stress ratios and post-welding technologies on fatigue strength of AH36 steel cross welded joints. The test results showed that the greater the stress ratio, the smaller the fatigue strength, and that the fatigue limit of the welded joint after ultrasonic treatment was significantly improved. Through S-N curve and microstructure analysis, Zhang et al. (2020) studied the fatigue properties of Q420 steel butt welds treated with three different welding processes (SMAW, SMAW+FCAW and SMAW+SAW). They found that the 1102 welded joint produced by SMAW primer + SAW filling cover was far better than the other two joints in fatigue performance.

The existing studies on the fatigue properties of welded steel mainly focus on low or high strength structural steel. Few are on the welding fatigue properties of medium strength Q420 steel with broad applicability. Moreover, the welded joints are mostly butt welding and non-load-bearing cross-fillet welding; cross-butt welding has not been studied. In addition, the fatigue test data of welded joints in current steel structure design need to be improved, so it is necessary to carry out fatigue test on Q420C steel welded joints.

In this work, the fatigue properties of three kinds of Q420C structural steel welded joints at room temperature were studied by experiments. The S-N curve of fatigue strength of the joints was fitted with the test data. In addition, the development of fatigue cracks is analyzed based on the fracture morphology, and the fatigue life of welded joints is compared with literature data and specification curves, which provides reference for the fatigue performance of Q420C structural steel welded joints.

2. Test Overview

2.1 Test materials

The Q420C steel used in this test was an 8mm thick steel plate. It meets the requirements of Chinese standard GB/T1591-2008 (2009). The chemical composition and melting analysis results of the steel plate are listed in Table 1. Manual arc welding was the welding method. Electric electrode was the Dongfeng SH·J557 fine grain steel manual electrode produced by Shanghai Welding Equipment Co., Ltd. The yield strength and tensile strength of the cladding metal were not less than 460 MPa and 550 MPa respectively, and its elongation was at least 17%.

Tab. 1 Melting analysis of Q420C steel plate (%)

Chemical compositions	C	Si	Mn	Cr	Mo	B	V	C_eq
Measured value	0.14	0.042	0.8	0.015	0	-	0	0.278
Factory value	0.07	0.19	1.08	0.02	0.004	-	0	-
Product standard	0.20	0.50	1.7	0.30	0.20	-	0.20	0.45

2.2 Specimen design

By referring to the relevant regulations in Test Methods for Cruciform Joins of Building Steel Structures (JG/T 288-2013,2013) and Metallic Materials—Fatigue Testing—Axial-Force-Controlled Method (GB/T3075-2008,2018), specimens with three kinds of welded joints were designed and fabricated, as shown in Fig. 1. The parameters adopted for the welding process are listed in Table 2. The connection types are shown in Figure 1: (a) butt-welded joint, (b) cross-butt-welded joint, and (c) cross-fillet-welded joint. The weld quality was tested by ultrasonic and radiographic testing, and it met the requirements of Code for Welding of Steel Structures (GB50611-2011, 2012). The butt-welded joint specimen was processed by wire cutting and the residual part of the weld was removed. The cross section is calculated by $A=15mm\times8mm=120mm^2$. The cross-butt-welded joint specimen was processed by wire cutting and the weld remained intact. The actual sizes of the four legs of the cross-fillet-welded joint were measured, which were averaged to be $h_f\approx5.7mm$. Corresponding effective cross-sectional area in strength calculation is $A_e=0.7h_f l_w=0.7\times5.7\times15mm^2=120mm^2$.
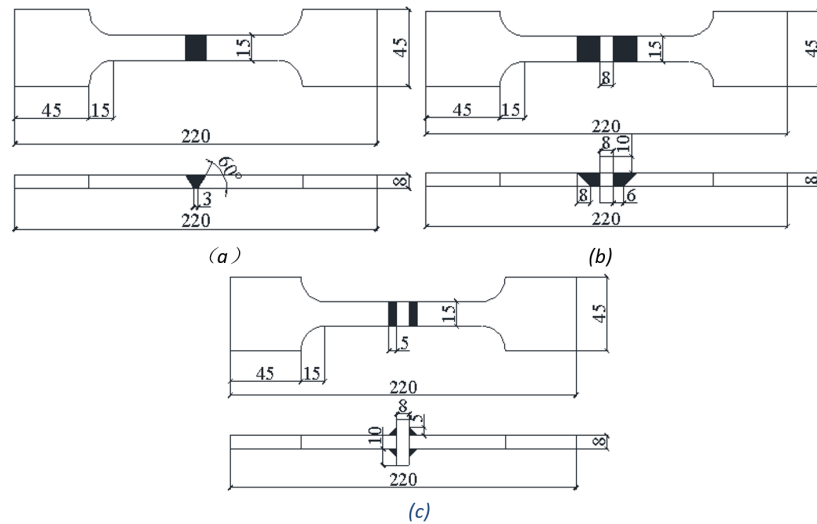
Fig. 1 Sample preparation(mm): (a) Butt-welded joint,(b) Cross-butt-welded joint,(c) Cross-fillet-welded joint.

Tab. 2 Welding parameters

Welding method	Diameter of electrode /mm	Welding current/A	Welding voltage/V	Welding speed/cm·min⁻¹
Manual arc welding	3.2	110	40	20~25

2.3 Test procedure

All specimens were subjected to monotonic tensile mechanical property test and tensile fatigue test on MTS fatigue testing machine. For each type of welding connection, 3 monotonic loading specimens and 12 cyclic loading specimens were designed, with a total of 45 specimens, as shown in Table 3. The monotone tensile test was controlled by displacement loading at a loading rate of 0.4 mm/min until the specimen was destroyed. The fatigue loading at room temperature was controlled by force at a frequency of 10Hz. The load waveform was alternating load of sinusoidal amplitude. The stress ratio was $R=P_{min}/P_{max}=0.1$. The value of P_{max} was calculated by kF_y, where k was the loading coefficient, and Fy was the yield load of the specimen. Considering that the load would not exceed 0.66 F_y under normal use (ANSI/AISC360-10, 2010), the initial value of k was 0.7 times the yield load F_y of monotonic tension. By adjusting the value of K for other specimens, the experiment ends until the number of cycles N reaches 2 million.

Tab. 3 Sample grouping

Connection type	Test type	Group type	Number
Butt-welded joint	Mechanical test	MDD	3
	Fatigue test	MDX	12
Cross-butt-welded joint	Mechanical test	SDD	3
	Fatigue test	SDX	12
Cross-fillet-welded joint	Mechanical test	SJD	3
	Fatigue test	SJX	12

3. Study on Fatigue Theory

From the point of view of fracture mechanics, fatigue failure is a process of gradual crack propagation. A large number of fatigue failure cases have been supported by the theory of linear elastic fracture mechanics. According to Paris, there is a log-linear relationship between the fatigue crack growth rate $\frac{da}{dN}$ and the stress intensity factor ΔK, known as the Paris law (Chen, 2005):

$$\frac{da}{dN} = C(\Delta K)^n \tag{1}$$

By integrating Eq. (1), the fatigue life expression when C and n are material-related constants can be obtained:

$$N = \frac{1}{C} \int_{a_1}^{a_2} \frac{da}{(\Delta K)^n} \tag{2}$$

where a_1 and a_2 are the initial crack size and the crack size at the end of the slow growth stage, respectively. The change of stress intensity factor $\Delta K = \alpha \sqrt{\pi a} \times \Delta \sigma$, where $\Delta \sigma$ is the stress variation range. $\Delta \sigma = S_{max} - S_{min} = S$, which is substituted into Eq. (2) to get:

$$N = (\Delta \sigma)^{-n} \left[\frac{1}{C} \int_{a_1}^{a_2} \frac{da}{(\alpha \sqrt{\pi a})^n} \right] \tag{3a}$$

$$N = \beta (\Delta \sigma)^{-n} \tag{3b}$$

$$\log N = \log \beta - n \log(\Delta \sigma) \tag{3c}$$

In the above equations, $\beta = 2 \left(C \pi^{3/2} \sqrt{a_1} \right)^{-1}$. The fatigue properties of materials are usually described by S-N relation.

$$\log S = A + B \log N \tag{4a}$$

$$S^m N = C \tag{4b}$$

where S is the nominal stress range of the section; N is the number of cycles of fatigue damage; m, A, B, and C are undetermined constants.

BS7608: 2014 is a standard for design and evaluation of fatigue resistance of steel structures based on nominal stress method and hot spot stress method established through fatigue test data of a series of welded joints. This standard is applicable to base materials with steel yield strength of 200~960 MPa and various welded joints. Fatigue assessment of various welded structures can be achieved through S-N curve. The fatigue types of components and connections stipulated in the BS7608 standard has 13 categories and grades. And the welded joints are divided into 12 design categories: B, C, D, E, F, F2, G, G2, Wl, S1, S2, and TJ according to details such as weld form, joint size, fatigue load direction, and crack initiation position (BS7608-2014, 2015). For each design category, the stress range Sr and the number of fatigue cycles N satisfy the following equation.

$$\log N = \log C_0 - dSD - m \log S_r \tag{5}$$

where N is the number of fatigue test results, S_r is the stress range in any one cycle, C_0 is the parameter defining the mean line S_r-N relationship, m is the inverse slope of $\log S_r$-$\log N$ curve, SD is the standard deviation of $\log N$, d is the number of standard deviation of $\log N$ from the mean S_r-N curve. Table 4 gives the values of BS7608 parameters corresponding to the three types of welded joints.

Tab. 4 Fatigue parameter value of BS7608

Connection type	Classes	Parameter C0	SD	m
Butt-welded joint	E	3.289×1012	0.2509	3
Cross-butt-welded joint	F2	1.231×1012	0.2279	3
Cross-fillet-welded joint	W1	2.5×1011	0.2140	3

In the *Standard for Design of Steel Structures* (GB50017-2017, 2017), the allowable stress design method based on the nominal stress is adopted for fatigue design calculation. The component and the connection are in an elastic state; the allowable stress amplitude depends on the types of component and the connection, the number of stress cycles, and the thickness of the plate. The fatigue checking calculation of the connections is carried out by formula (6), and the values of the parameters in the formula are shown in Table 5.

$$\Delta\sigma \leq [\Delta\sigma] \tag{6}$$

$$[\Delta\sigma] = (C/N)^{1/\beta} \tag{7}$$

Tab. 5 Fatigue paramete value of GB50017

Connection type	Classes	Parameter C	Parameter β
Butt-welded joint	Z2	861×1012	4
Cross-butt-welded joint	Z6	1.46×1012	3
Cross-fillet-welded joint	Z8	0.72×1012	3

The ANSI/AISC360-10 standard subdivides the fatigue calculation stress categories of base materials, welded joints, bolts and screws into A, B, B', C, C', C'', D, E, F, and G (ANSI/AISC360-10, 2010). The allowable stress amplitudes of the three kinds of connections in this paper are given by the corresponding formulae below.

$$F_{SR} = \begin{cases} \left(\frac{C_f \times 329}{N}\right)^{0.333} B\,(\text{Butt} - \text{welded joint}) \\ \left(\frac{14.4\times10^{11}}{N}\right)^{0.333} C\,(\text{Cross} - \text{butt} - \text{welded joint}) \\ R_{FIL}\left(\frac{14.4\times10^{11}}{N}\right)^{0.333} C''(\text{Cross} - \text{fillet} - \text{welded joint}) \end{cases} \tag{8}$$

$$R_{FIL} = \left(\frac{0.10 + 1.24(\omega/t_p)}{t_p^{0.167}}\right) \leq 1.0 \tag{9}$$

where F_{SR} is the allowable stress amplitude, N is the number of stress cycles, C_f is the fatigue category constant whose value is 120×10^8, R_{FIL} is the reduction factor of the joint's transverse fillet weld on both sides, ω is the size of leg, whose value is 5 mm, and t_p is the thickness of the tensile plate and its value is 8mm.

In the test on the three connection types, the stress range $\Delta\sigma$ is calculated according to the stress ratio 0.1, i.e. $R=P_{max}/P_{min}=S_{max}/S_{min}=0.1$. Thus, $\Delta\sigma=0.9S_{max}=S$. Then the S-N relationship in Table 6 is obtained by substituting the parameters of various standards into the corresponding formulae.

Tab. 6 S-N relationship

Connection type	BS7608: 2014	GB50017-2017	ANSI/AISC360-10
Butt-welded joint	$S=14857.29N^{(-1/3)}$	$S=5419.92N^{-0.25}$	$S=15652.89N^{-0.333}$
Cross-butt-welded joint	$S=10707.39N^{(-1/3)}$	$S=11333.88N^{(-1/3)}$	$S=11187.54N^{-0.333}$
Cross-fillet-welded joint	$S=6294.15N^{(-1/3)}$	$S=8954.64N^{(-1/3)}$	$S=6917.13N^{-0.333}$

4. Test Results

4.1 Tensile mechanical properties

The control axial force kF_y of the fatigue test was determined according to GB/T3075-2008. Therefore, tensile mechanical performance test was carried out on the welded joint specimens to determine F_y. The load-displacement relationship curves obtained from the tensile tests of the three types of weld connections are shown in Figure 2, and the test results of each specimen are presented in Table 7.
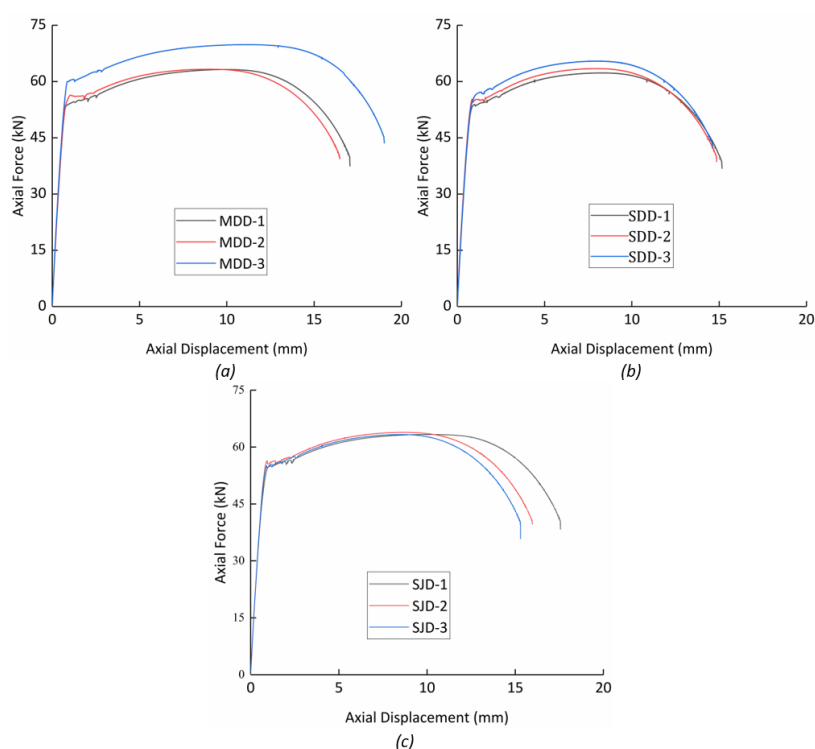

Fig. 2 Monotonic tensile load displacement curve: (a) Butt-welded joint, (b) Cross-butt-welded joint, (c) Cross-fillet-welded joint.

Tab. 7 Tensile test results

Connection type	Specimen number	F_y/kN	F_u/kN	f_y/MPa	f_u/MPa	F_y/F_u
Butt-welded joint	MDD-1	54.5	63.2	454.2	526.7	0.86
	MDD-2	57.5	63.1	479.2	525.8	0.91
	MDD-3	60.5	69.7	504.2	580.8	0.87
	average	57.5	65.3	479.2	544.2	0.88
Cross-butt-welded joint	SDD-1	54.0	62.3	450.0	519.2	0.87
	SDD-2	55.2	63.4	460.0	528.3	0.87
	SDD-3	58.0	65.4	483.3	545.0	0.89
	average	55.7	63.7	464.2	530.8	0.87
Cross-fillet-welded joint	SJD-1	55.0	63.3	458.3	527.5	0.87
	SJD-2	56.3	63.6	469.2	530.0	0.89
	SJD-3	55.2	63.9	460.0	532.5	0.86
	average	55.5	63.6	462.5	530.0	0.87

The primary tensile failure positions of the three types of weld connection specimens are all near the arc transition section of the specimens, basically the same as the failure position of the base metal specimen under the same conditions, and there is no tensile failure of the welds. These indicate that the weld joints meet the design requirements of equal strength. The tensile fractures of all specimens show typical plastic deformation characteristics. The differences of fracture yield and ultimate load among three kinds of joint specimens are less than 5%, and the yield strength ratio is about 0.87. These imply that the welding quality of the specimens meets the requirements, and the tensile failure strength mainly depends on the properties of the base material. The load-displacement relationship curve of the specimen can be divided into the elastic stage, the yield stage, the strengthening stage and the failure stage, consistent with the tensile failure of the low-alloy high-strength steel base material.

4.2 Fatigue test results

The axial force of fatigue loading of welded joint specimens is based on the average yield load obtained from tensile test in Table 7. The average yield load of all kinds of welded joints is 57.5kN, and the fatigue performance tests under different loading factors K are taken into account. The results are shown in Table 8, 9 and 10. The fatigue failure positions of the three types of specimens are all at the weld connection. It shows that the fatigue failure of welded joint specimens caused by the inhomogeneity, geometric discontinuity, and residual stress of the weld or by the unavoidable defects during in the welding all appear at the welding seam.

Tab. 8 Fatigue test parameters and results of butt-welded joint

| Specimen number	K	S_{max} /MPa	F /Hz	S /MPa	N/cycle
MDX-1	0.62	297.08	10	267.38	1625182
MDX-2	0.70	335.42	10	301.88	157084
MDX-3	0.68	325.92	10	293.33	380915
MDX-4	0.60	287.50	10	258.75	1432011
MDX-5	0.65	311.46	10	280.31	458116
MDX-6	0.58	277.92	10	250.13	1828264
MDX-7	0.62	297.08	10	267.38	703875
MDX-8	0.60	287.50	10	258.75	1669477
MDX-9	0.55	263.54	10	237.19	1953255
MDX-10	0.70	335.42	10	301.88	241907
MDX-11	0.66	316.25	10	284.63	382975
MDX-12	0.63	301.88	10	271.69	945216

Tab. 9 Fatigue test parameters and results of cross-butt-welded joint

Specimen number	K	S_{max} /MPa	F /Hz	S/MPa	N /Cycle
SDX-1	0.70	335.42	10	301.88	26561
SDX-2	0.60	287.50	10	258.75	58686
SDX-3	0.55	263.54	10	237.19	38878
SDX-4	0.45	215.63	10	194.06	120228
SDX-5	0.40	191.67	10	172.50	241913
SDX-6	0.30	143.75	10	129.38	662669
SDX-7	0.28	134.17	10	120.75	456426
SDX-8	0.25	119.79	10	107.81	1052318
SDX-9	0.22	105.42	10	94.88	2000000
SDX-10	0.24	115.00	10	103.50	2000000
SDX-11	0.27	129.38	10	116.44	1075740
SDX-12	0.23	95.83	10	86.25	980012

Tab. 10 Fatigue test parameters and results of cross-fillet-welded joint

Specimen number	K	S_{max} /MPa	F /Hz	S/MPa	N /Cycle
SJX-1	0.25	119.79	10	107.81	515925
SJX-2	0.22	105.42	10	94.88	379449
SJX-3	0.20	95.83	10	86.25	2000000
SJX-4	0.28	134.17	10	120.75	186346
SJX-5	0.19	91.04	10	81.94	2000000
SJX-6	0.21	100.63	10	90.56	1734188
SJX-7	0.24	115	10	103.50	1094757
SJX-8	0.26	124.58	10	112.13	914886
SJX-9	0.27	129.38	10	116.44	1184697
SJX-10	0.30	143.75	10	129.38	277720
SJX-11	0.29	138.96	10	125.06	322692
SJX-12	0.23	110.21	10	99.19	480348

After analyzing the test data, it is found that the results of data points MDX-7, SDX-7, SDX-12, SJX-2 and SJX-4 deviate significantly from the overall result, so they will be discarded as abnormal data in the analysis. The logarithmic linear relationship between the stress range S and the number of cycles N is obtained by fitting of the test data with reference to Eq. (4a). The P-S-N relationships of 0.95 survival rate can also be obtained. The fitting S-N curves in logarithmic coordinates are shown in Figure 3 The S-N relationships of the three types of welds are listed in Table 11.
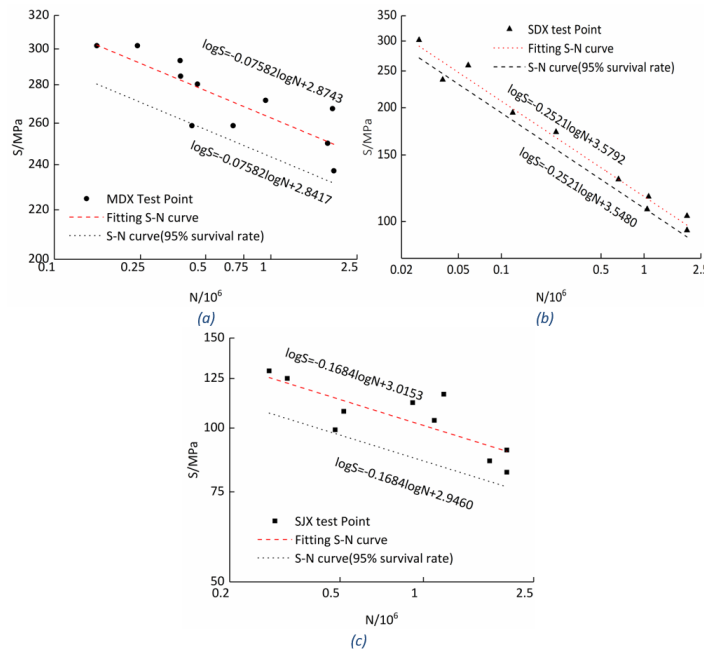
Fig. 3 Fitting S-N curve in logarithmic coordinates: (a) Butt-welded joint, (b) Cross-butt-welded joint, (c) Cross-fillet-welded joint.

Tab. 11 Fitting S-N equation

Type	General form		Logarithmic form	
	S-N equation	95% S-N equation	S-N equation	95% S-N equation
MDX series	S=748.69N-0.07582	S=694.541N-0.07582	logS=2.8743-0.07582logN	logS=2.8417-0.07582logN
SDX series	S=3794.90N-0.2521	S=3531.83N-0.2521	logS=3.792-0.2521logN	logS=3.5480-0.2521logN
SJX series	S=1035.86N-0.1684	S=883.08N-0.1684	logS=3.0153-0.1684logN	logS=2.9460-0.1684logN

The fitting results of test data are compared with the S-N curves of corresponding connection fatigue life stipulated by various standards, as shown in Figure 4. The ultimate fatigue strength of the three connections under the action of 2 million stress cycles is compared with the standard value, as shown in Table 12.
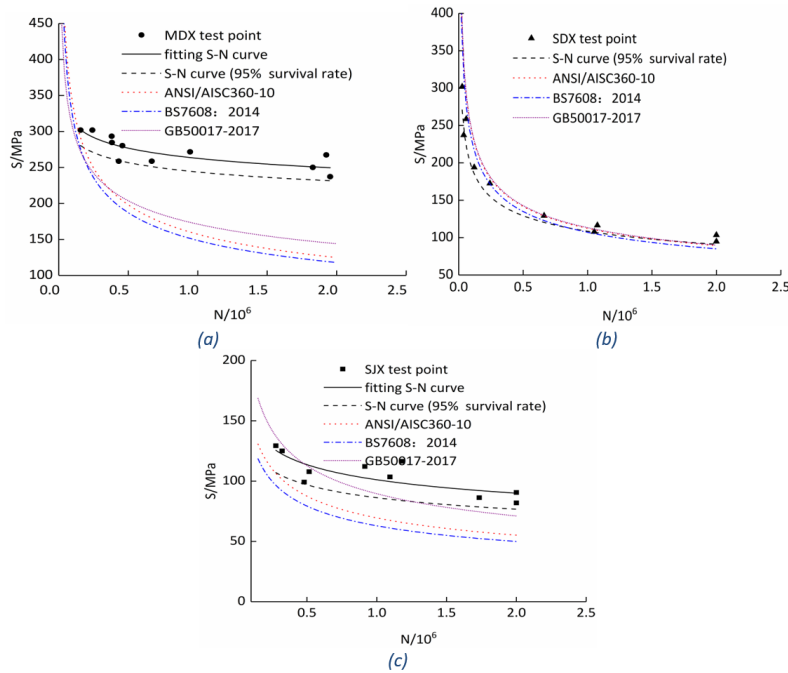

Fig. 4 Contrast S-N curves in Cartesian coordinates: (a) Butt-welded joint, (b) Cross-butt-welded joint, (c) Cross-fillet-welded joint.

**Tab. 12** Comparison of fatigue limit strength

Connection type	S /MPa				
	Fitted value	95% survival	BS7608: 2014	GB50017-2017	ANSI/AISC360-10
Butt-welded joint	249.2	231.2	117.9	144.1	124.8
Cross-butt-welded joint	97.9	91.1	85	90	89.2
Cross-fillet-welded joint	90	76.7	50	71.1	55.2

From the fitting and calculation results of the test data, it can be known:

1. The values of MDX sample fitting curve and 95% survival rate curve are much larger than the values corresponding to BS7608: 2014, GB50017-2017 and ANSI/AISC360-10 standard curves. Among them, the fatigue limit of the 95% survival rate corresponding to 2×10^6 stress cycles is 1.96 times the calculated value of BS7608: 2014, 1.6 times the calculated value of GB50017-2017, and 1.85 times the calculated value of ANSI/AISC360-10. The calculated values of the standard curves also deviate significantly. After the number of stress cycles exceeds 180,000 times, the calculated value of GB50017-2017 is greater than that of BS7608:2014, and after it exceeds 360,000, the calculated value of GB50017-2017 is greater than that of ANSI/AISC360-10. On the whole, BS7608:2014 calculated value is the most conservative, while GB50017-2017 calculated value is closer to the fitting curve.

2. The SDX sample fitting curve and 95% survival rate curve are close to the standard curves, and the difference among the standard curves is quite small. Before the number of stress cycles reaches 0.86 million, 1.7 million and 1.54 million, the 95% survival rate curve is higher than BS7608:2014, GB50017-2017 and ANSI/AISC360-10 curves. At 2×10^6 stress cycles, the fatigue limit of 95% survival rate is respectively 8.1%, 2.1%, and 3.0% higher than the calculated values of BS7608:2014, GB50017-2017 and ANSI/AISC360-10.

3. The SJX sample fitting curve and 95% survival rate curve are closer to GB50017-2017 curve; BS7608:2014 and ANSI/AISC360-10 curves are more conservative. After the number of stress cycles exceeds 1.26 million, the 95% survival rate curve is higher than the GB50017-2017 curve. The fatigue limit of 95% survival rate corresponding to 2×10^6 stress cycles is 53.4%, 7.9%, and 38.9% higher than the calculated values of BS7608: 2014, GB50017-2017 and ANSI/AISC360-10, respectively.

4.3 Fracture analysis

The fracture positions of all kinds of specimens under fatigue test are at the weld joint. MDX-6 specimen was damaged after 1828264 stress cycles under load of 250.1 MPa; SDX-7 specimen was damaged under the load of 116.4 MPa after 456426 stress cycles; SJX-1 specimen broke down under the load of 107.8 MPa after 515925 stress cycles. The typical macroscopic fractures of the specimen are shown in Figure 5. All the fractures have typical characteristics of fatigue fracture, and they are grouped into crack initiation zone I, crack propagation zone II and final fast fracture zone III. The cracks of welded joint are generally initiated in the heat-affected zone or near the fusion zone. The fracture surface of the specimen before instant fatigue failure is flat and smooth. The instantaneous fracture zone is rough, consistent with the obvious characteristic appearance of the coarse particles in plastic deformation.

*(a)*   *(b)*   *(c)*
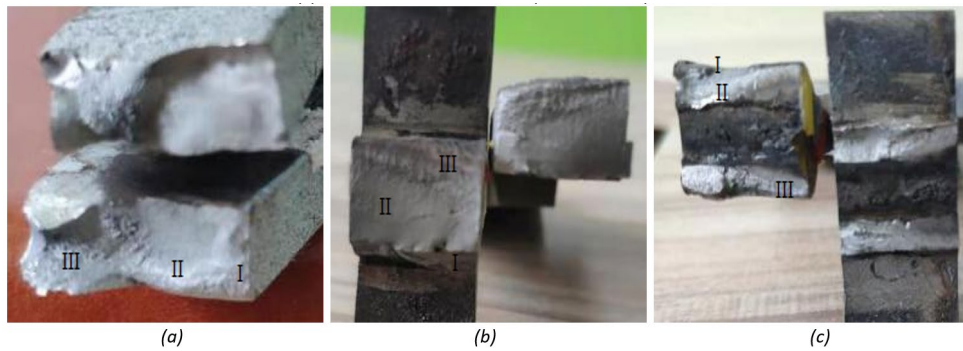
Fig. 5 Fatigue Fracture of Specimens: (a) Butt-welded joint (MDX-6), (b) Cross-butt-welded joint (SDX-7), (c) Cross-fillet-welded joint (SJX-1).

A Hitachi S-4800 scanning electron microscope was used to scan the microscopic morphology of the fractures of the above three specimens. The results are shown in Figures 6,7 and 8. The fractures of the specimens were magnified by 50 times, 500 times and 1000 times to observe the three boundary areas of the fracture. Images in (a) show the crack initiation: the inherent defects of fatigue crack can be found under 50 times of magnification. Images in (b) show the crack propagation: the fatigue streaks caused by cyclic loading and the secondary cracks caused by asynchronous crack propagation are observed under 500 times of magnification. Images in (c) show the final fast fracture: after 1000 times of magnification, dimples of varying sizes can be observed, showing the rapid expansion of material damage.

(a)   *(b)*

(c)
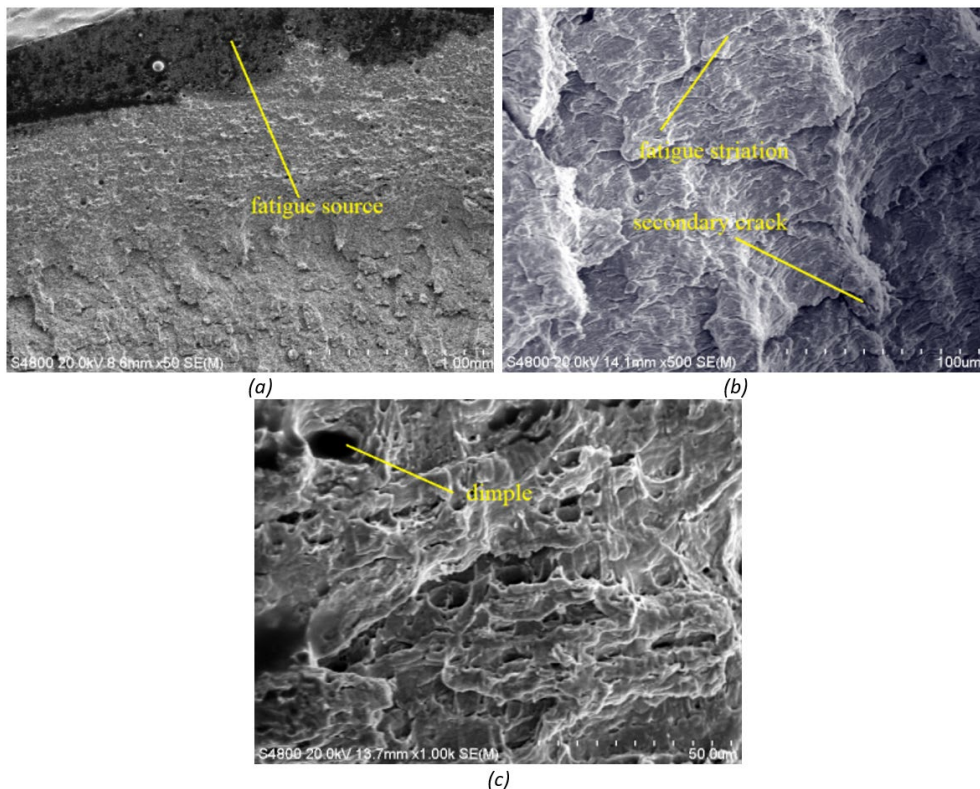
Fig. 6 Fracture morphology of butt-welded joint (MDX-6): (a) The crack initiation, (b) The crack propagation, (c) The final fast fracture.

(a)   (b)

(c)
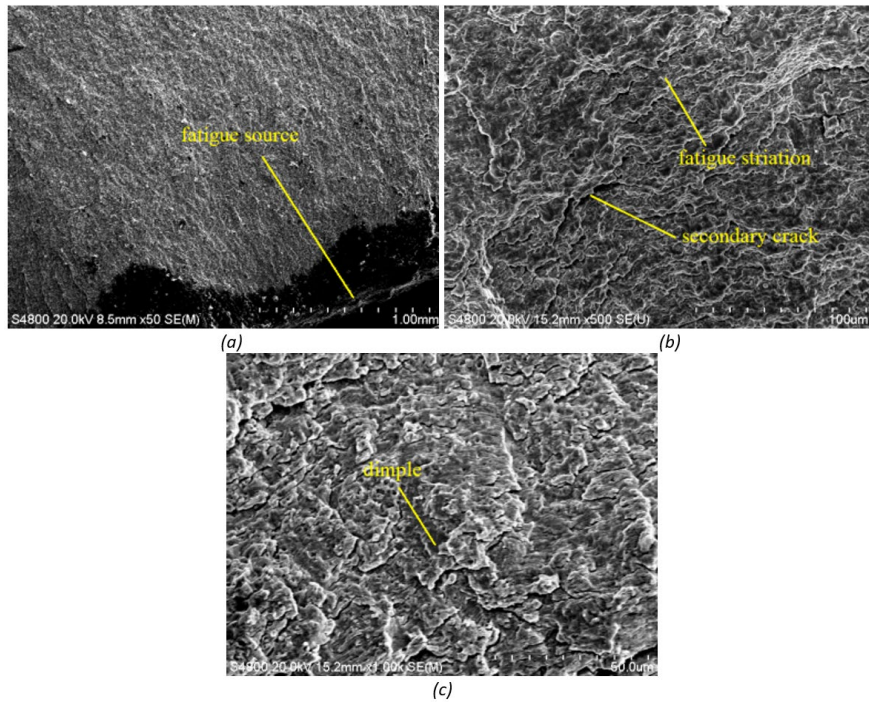
Fig. 7 Fracture morphology of cross-butt-welded joint (SDX-7): (a) The crack initiation, (b) The crack propagation, (c) The final fast fracture.

(a)   (b)

(c)
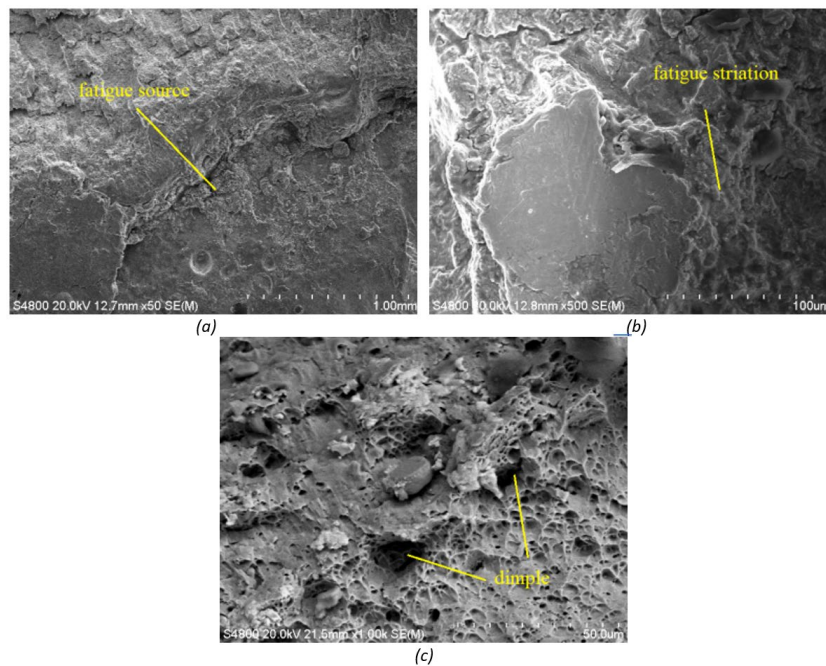
Fig. 8 Fracture morphology of cross-fillet-welded joint (SJX-1): (a) The crack initiation, (b) The crack propagation, (c) The final fast fracture.

4.4 Fatigue displacement analysis

The fatigue test was set to stop when the specimen breaks down or when the number of stress cycles reaches 2 million. Due to the small cyclic stress, the displacement of unbroken specimens during fatigue loading was small and the maximum value basically remained unchanged. The fatigue displacement of fractured specimens varying with the ratio of N to N_f is shown in Figure 9. In this figure, δ is the displacement of the specimen under load, N is the number of loading cycles, and N_f is the fatigue life of specimen. As shown in Figure 9, the displacement change processes of the four typical specimens correspond to the two stages of crack propagation zone II and instantaneous fracture zone III. The crack initiation zone I, the crack initiation stage, is directly skipped. This is consistent with the fatigue factures of the specimens.
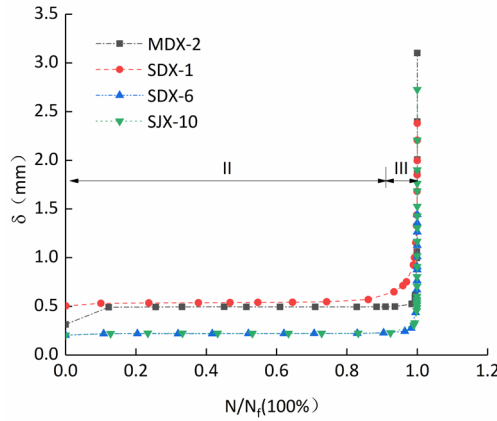
Fig. 9 Fatigue displacement curve.

When the ratio of N/N_f is below 0.9, MDX-2 and SDX-1 specimens have the maximum fatigue displacement of 0.5 mm under the action of 301.88 MPa ultimate stress; SDX-6 and SJX-10 specimens have the maximum fatigue displacement of 0.2 mm under the action of 129.38 MPa ultimate stress. The displacement of all specimens under load is basically proportional to the applied load, and the extreme displacement in the crack propagation zone remains unchanged. When the ratio of N/N_f is larger than 0.9, the specimen enters the instantaneous fracture zone, and the remaining uncracked part shows obvious plastic deformation, and the displacement starts to increase rapidly until the specimen fractures.

5. Fatigue Damage Analysis

Fatigue failure can be seen as the phenomenon of gradual damage or even fracture of materials or connections under cyclic loading. The fatigue damage theory can estimate the remaining service life based on the service conditions of the engineering structure. Under a given cyclic load, the damage variable remains constant during a stress cycle. In high-cycle fatigue, the number of cycles N, the damage variable D and the fatigue life N_f satisfy Eq. (10). And the fatigue life N_f can be calculated by Eq. (11) under uniaxial tension fatigue conditions (Lou, 1991).

$$D = 1 - \left(1 - \frac{N}{N_f}\right)^{1/(\beta+2)} \tag{10}$$

$$N_f = \frac{(\beta+1)\left(S_{max}^{\beta+1} - S_{min}^{\beta+1}\right)^{-1}}{2B(\beta+2)} \tag{11}$$

where S_{max} and S_{min} are the maximum and minimum stresses under cyclic loading, and B and β are material constants, which can be determined by fatigue tests.

According to the fatigue test in Table 11, the β values of MDX, SDX and SJX specimens can be obtained by fitting the S-N power function relationship, which are 12.1891, 2.9667, and 4.9382, respectively. The fatigue damage curves are obtained by substituting the β value into Eq. (10), as shown in Figure 10.
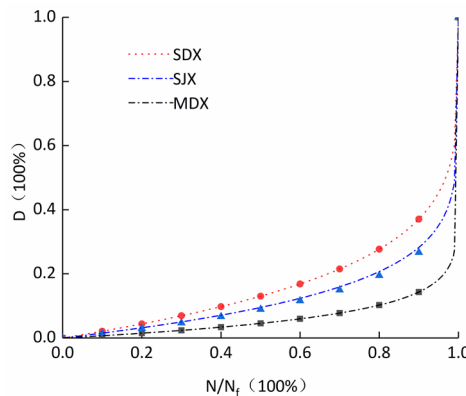

Fig. 10 Fatigue damage curve.

It can be seen from Figure 10 that when N/N$_f$<0.5, the damage variable D increases slowly as the cycle ratio approaches a linear relationship, and crack bands with roughly constant spacing can be observed in the crack propagation zone. When 0.5<N/N$_f$<0.9, the damage variable D increases rapidly and non-linearly with the N/N$_f$ ratio, and the crack band spacing in the crack propagation zone gradually increases. When N/N$_f$>0.9, the damage variable D approaches 1 with the increasing N/N$_f$ ratio, and the specimens enter the instantaneous fracture stage. Before the specimens fracture, the cumulative damage index of MDX specimen is about 25%, followed by SJX specimen (50%) and SDX specimen (60%). It is therefore can be concluded that the damage development rate of MDX is the slowest, followed by SJX and SDX successively. The reason may be that the stress concentration at the weld joints is different. The removal of the excess height after welding the MDX specimen reduces the effect of stress concentration.

6. Comparative Analysis of Joint Fatigue

Extensive studies have been carried out on the fatigue test of welded joints, and most of them focus on butt-welded joints and cross-butt-welded joints. However, there are few comparative analyses of the fatigue test results. It is difficult to compare the fatigue tests due to the large number of loading parameters, different stress calculation methods, and inconsistent fitting variables. The loading parameters involved in fatigue test usually include the maximum stress, stress ratio, stress range, stress amplitude, load waveform and loading frequency. As for the calculation of the cross-sectional stress of specimen, most tests use the nominal cross-sectional area, and some tests use the actual cross-sectional area. In addition, the stress S of S-N curve fitting is often confused. In some tests, the maximum stress S$_{max}$ is adopted, while the stress range or stress amplitude is used in some other.

In this paper, the S-N curves of some references are compared while retaining their original experimental data (Guo et al., 2018a; Guo et al., 2018b; Guo et al., 2018c; Shi et al., 2014a; Shi et al., 2014b; Zong et al.,2017a). In the S-N curve, S represents the stress range, and the stress ratio in the cited literature is all 0.1. The steel types, plate thicknesses and fitting curves of test points are shown in Figure 11. It can be known from Figure 11 that the test data of various welded joints are quite disperse, and that most of the test points are distributed above the standard curve. It indicates that the fatigue design of typical welds according to the standard curve can meet engineering requirements. The fatigue properties of similar welded steel joints with varying strength grades are close, implying that the strength grade of steel has little impact on the fatigue performance of joints. The test value of cross-fillet-welded joint with a plate thickness of 12 mm is obviously lower than that with a plate thickness of 8 mm, indicating that the fatigue performance of connection becomes worse with the increasing plate thickness. There are few studies on the fatigue performance of other types of welded joints, like butt-welded joints, in the standards. Thus, more fatigue tests or theoretical studies on other connections should be carried out to improve the standards.
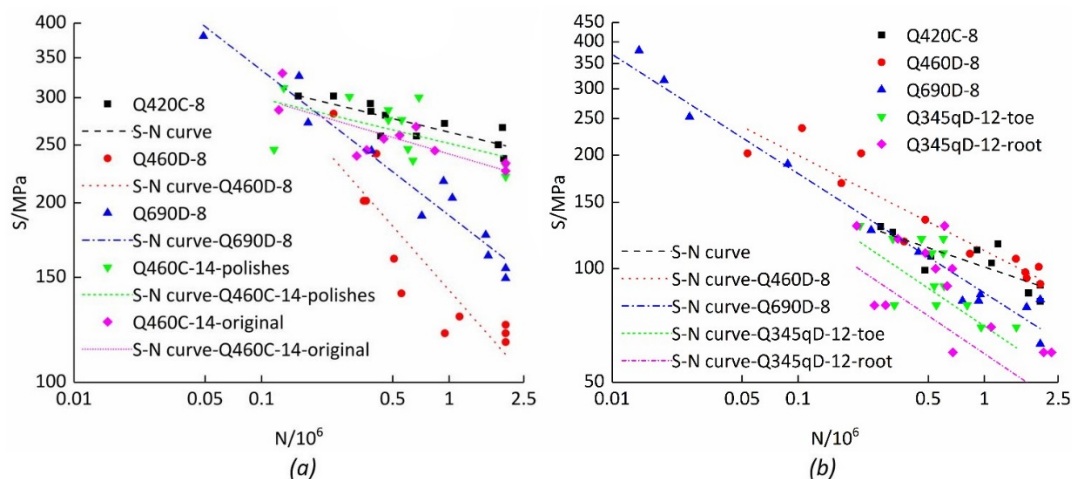

Fig. 11 Contrast S-N curves in Cartesian coordinates: (a) Butt-welded joint, (b) Cross-fillet-welded joint.

7. Conclusions

The following conclusions are drawn from the experimental study on the fatigue properties of three typical welded joints of 8 mm thick Q420C steel plate: butt-welded joints, cross-butt-welded joints, and cross-fillet-welded joints.

1. The specimens all showed typical fatigue failure characteristics. The fracture was mainly distributed across the crack propagation zone and the instantaneous fracture zone. There were clear fatigue crack bands in the crack propagation zone, and the fracture of the instantaneous fracture zone was consistent with the plastic tensile fracture.

2. The values of fitting curve of butt-welded joint and the 95% survival rate curve are much larger than those of BS7608: 2014, GB50017-2017 and ANSI/AISC360-10 standard curves, indicating a large safety margin. It is therefore suggested to moderately increase the standard value.

3. The fitting curve of cross-butt-welded joint agreed well with the standard curves, and the difference among the three standard curves was quite small, indicating a small safety margin of the standards. It is necessary to increase the fatigue test research of cross-butt-welded joint and have similar safety reserve with other weld joints.

4. The fitting curve of cross-fillet-welded joint and 95% survival rate curve were closer to GB50017-2017 curve. When the number of stress cycles was below 1.26 million, the test values were smaller than the calculated value of 95% survival rate, and BS7608: 2014 and ANSI/AISC360-10 curves were more conservative.

5. The comparison between cross-fillet-welded joints of 12 mm and 8 mm steel plates showed that the fatigue performance of joints became worse with the increasing thickness of plate. In the future research, finite element numerical simulation can be used to quantify the impact of steel plate thickness on joint fatigue performance. At the same time, the experimental and theoretical research on the fatigue performance of other joints can be conducted.

Acknowledgements

Author's Contribuitions: Conceptualization,Yongming Xing ; Investigation,Liguo Yang ; Writing - original draft,Liguo Yang; Writing - review & editing, Yongming Xing and Liguo Yang; Funding acquisition,Yongming Xing ; Resources, Liguo Yang.

Editor: Marcílio Alves

References

ANSI/AISC360-10 (2010) Specification for Structural Steel Buildings. ANSI/AISC360-10,American Institute of Steel Construction, Chicago IL, USA.

BS7608-2014 (2015) Guide to fatigue design and assessment of steel products: BS7608-2014, British standards Institution, London, UK.

Chen SF (2005) Principle of steel structure design,3rd edition, Science Press, Beijing, CHN (in Chinese).

Cheng F, Hu CS, Wang JS, Guo N, Wu HY, Li ZR, Zhang DC (2017) Experimental research on fatigue behavior of Q420 high strength steel, Steel Construction 32(11):12-15(in Chinese).

Custafsson M (2002) Thickness effect in fatigue of welded extra high strength steel joints, Proceedings of the Eighth International Fatigue Congress, Stockholm, Sweden, 205-224.

GB50017-2017 (2017) Code for design of steel Structures GB50017-2017, Planning Press, Beijing, CHN (in Chinese).

GB50611-2011 (2012) Code for welding of steel structures,China Construction Industry Press, Beijing, CHN (in Chinese).

GB/T1591-2008 (2009)High strength Low alloy structural steels, China Standard Press, Beijing, CHN (in Chinese).

GB/T3075-2008 (2008) Metallic materials-Fatigue testing-Axial force controlled method, China Standard Press, Beijing, CHN (in Chinese).

Guo HC, Hao LP, Li YL, Liu YH, Wan JH (2018a) Experimental study on fatigue Performance of Q460D high-strength steel and its welded joints, Journal of Building Structures 39(8):157-164(in Chinese).

Guo HC, Wan JH, Liu YH, Hao JP (2018b) Experimental study on fatigue performance of high strength steel welded joints, Thin Walled Structures 131:45-54.

Guo HC, Wan JH, Liu YH,Wang DF (2018c) Experimental study on fatigue Performance of Q690D high strength steel welded joints, China Civil Engineering Journal 51(9):1-9(in Chinese).

Janosch JJ, Koneczny H, Debiez S, Statnikov, EC, Troufiakov VJ, Mikhee PP (1996) Improvement of fatigue strength in welded joints (in HSS and in aluminium alloys) by ultrasonic hammer peening Welding in the World 37 (1)72-83.

JG/T 288-2013 (2013) Test methods for cruciform joints of building steel structures, China Standard Press, Beijing, CHN (in Chinese).

Jia DF, Wang YQ, Cui J, Liao XW, Gu HY (2017) Experimental research on fatigue performance and fracture mechanism of Q345qD butt welds. Industrial Construction 47(11)175-180 (in Chinese).

Lei HG, Fu Q, Liu XJ (2010) Research progress of steel structure fatigue in past 30 years in China. Journal of Building Structures (Supplementary Issue 1) 31(SI)84-91 (in Chinese).

Leitner M,Stoschka M, Schorghuber M, Eichlseder W (2011) Fatigue behavior of high-strength steels using an optimized welding process and high frequency peening technology, IIW International Conference, International Institute of Welding, Chennai, India,17-22.

Lou ZW (1991) Damage mechanics foundation, Xi'an Jiaotong University Press, Xi'an Shaanxi Province, CHN (in Chinese).

Okawa T, Shimanuki H, Funatsu Y, Nose T, Sumi Y (2013)Effect of preload and stress ratio on fatigue strength of welded joints improved by ultrasonic impact treatment, Welding in the World 57:235-241.

Shi G, Zhang JX (2014a) Fatigue Performance test study on high strength steel Q460C and its welded connection, Building Structure 44(17):1-6 (in Chinese).

Shi G, Zhang JX (2014b) Fatigue test of high strength steel Q460D, Industrial Construction 44(3):6-10(in Chinese).

Weich I (2008) Fatigue behavior of mecnical post welds treated weld depending on the edge layer condition PHD Thesis, Technischen Universitat Carolo-Wilhelmina, Braunschweig.

Zhang YF, Chen Z, Liu GH (2020) Study on fatigue property of Q420 steel with different welding process, Welding Technology 49(6):13-17(in Chinese).

Zong L, Shi G, Wang YQ, Yan JB, Ding Y (2017a)Investigation on fatigue behavior of load-carrying fillet welded joints based on mix-mode crack propagation analysis. Archives of Civil and Mechanical Engineering 17:677-686,

Zong L, Shi G, Wang YQ, Li ZX, Ding Y (2017b) Experimental and numerical investigation on fatigue performance of non-load-carrying fillet welded joints, Journal of Constructional Steel Research 130:193-201.